Chemistry Research Journal, 2022, 7(2):6-28

Available online www.chemrj.org

Research Article

ISSN: 2455-8990
CODEN(USA): CRJHA5

A DFT analysis of the relationships between electronic structure and activity at D_2, 5-HT_{1A} and 5-HT_{2A} receptors in a series of Triazolopyridinone derivatives

Juan S. Gómez-Jeria[1,2]*, Andrés Robles-Navarro[1], Ignacio Jaramillo-Hormazábal[1]

[1]Quantum Pharmacology Unit, Department of Chemistry, Faculty of Sciences, University of Chile. Las Palmeras 3425, Santiago 7800003, Chile.
[2]Glowing Neurons Group, CP 8270745 Santiago, Chile
* facien03@uchile.cl

Abstract The Klopman-Peradejordi-Gómez FQSAR method was applied to search for relationships between the electronic structures of a group of triazolopyridinone derivatives and their activities at the dopamine D_2 receptor and the serotonin 5-HT_{1A} and 5-HT_{2A} receptors. The electronic structure was calculated with Density Functional Theory at the B3LYP/6-31G(d,p) level after full geometry optimization. D-Cent-QSAR software was employed for obtaining all the local atomic reactivity indices. Statistically significant equations were found for the three receptors. The results suggest that atoms engage in halogen, non-classical weak carbon hydrogen bonds, electrostatic and alkyl or alkyl-π interactions.

Keywords KPG QSAR model, Klopman-Peradejordi-Gómez method, Triazolopyridinone, D_2 receptor, 5-HT_{1A} receptor, 5-HT_{2A} receptor, atypical antipsychotics, antipsychotic therapy, receptor selectivity, local atomic reactivity indices

Introduction

The second-generation antipsychotics (also called atypical antipsychotics, AAs) are a group of molecules employed to treat agitation associated with dementia, anxiety disorder, autism spectrum disorder, bipolar disorder, and schizophrenia. Clozapine is the first atypical antipsychotic. Interestingly, this molecule can bind dopamine (D_1, D_2, D_3, D_4), serotonin (5-HT_{1A}, 5-HT_{1B}, 5-HT_{2A}, 5-HT_{2C}, 5-HT_6, 5-HT_7), adrenergic (α_1, α_2), muscarinic (M_1, M_3) and histamine (H_1) receptors. The antipsychotic effects occur primarily through antagonism at D_2 dopamine receptor (the overactive dopaminergic activity on D_2 receptors in the mesolimbic pathway is accountable for the positive symptoms of schizophrenia). "When 5-HT_{2A} antagonistic agents occupy 5-HT_{2A} receptors in the mesocortical pathway and in the prefrontal cortex, the negative symptoms of schizophrenia, affective symptoms, and cognitive deficits and abnormalities are treated and reduced. Furthermore, 5-HT_{2A} receptor antagonism blocks the serotonergic excitation of cortical pyramidal cells, reducing glutamate release, which in turn lowers hyperactive dopaminergic D_2 receptor activity in the mesolimbic pathway, reducing or eliminating the positive symptoms of schizophrenia" [1].
Then, AAs with dual antagonistic properties at the D_2 and 5-HT_{2A} receptors have a partial effectiveness in ameliorating negative symptoms and cognitive deficits. In addition, "some effects of 5-HT_{1A} receptor activation

include decreased aggressive behavior/ideation, increased sociability, and decreased anxiety and depression" [1]. Then, an agonistic effect at the 5-HT_{1A} receptor is beneficial for the amelioration of current antipsychotic therapy.

Therefore, new molecules with an antagonistic activity at the D_2 and 5-HT_{2A} receptors and an activating activity at the 5-HT_{1A} receptor are highly desirable to increase our knowledge and to obtain new molecules with increased activity and selectivity [2-12]. In out Unit we have recently analyzed the D_1 and D_2 receptor binding affinities of a group of (S)-enantiomers of 11-(1,6-dimethyl-1,2,3,6-tetrahydropyridin-4-yl)-5*H*-dibenzo[b,e][1,4] diazepines to be used as possible atypical antipsychotics [13]. In previous studies, we have analyzed the D_2, 5-HT_{1A} and 5-HT_{2A} receptor affinity of other molecules possessing biological activity [14-25].

Recently, Wang et al. reported the activity of a series of triazolopyridinone derivatives at the D_2, 5-HT_{1A} and 5-HT_{2A} receptors [6]. Their data was of enough interest to use it to search relationships between electronic structure and activity. Here we report the results of this work.

Methods, Models and Calculations

Biological Activities

The selected molecules are a series of triazolopyridinone derivatives possessing an inhibitory activity against the D_2 and 5-HT_{2A} receptors and an agonistic activity at the 5-HT_{1A} receptor (they were measured with using HTRF cAMP and FLIPR calcium assays) [6]. The molecules are depicted in Fig. 1 and the activities are summarized in Table 1.

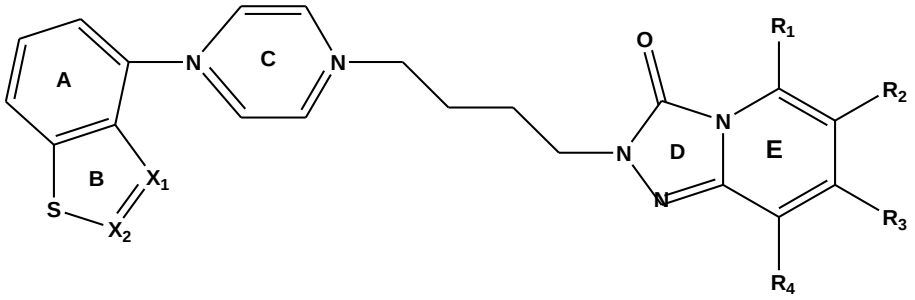

Figure 1: General formulas of Triazolopyridinone derivatives

Table 1: Triazolopyridinone derivatives and biological activities

Mol.	X_1	X_2	R_1	R_2	R_3	R_4	log(IC_{50}) D_2	log(EC_{50}) 5-HT_{1A}	log(IC_{50}) 5-HT_{2A}
1	CH	CH	H	H	H	H	1.09	0.23	1.53
2	CH	CH	H	F	H	H	1.42	-1.00	1.67
3	CH	CH	H	H	H	F	1.48	0.26	1.55
4	CH	CH	H	F	H	F	1.80	0.08	1.43
5	CH	CH	H	Cl	H	H	2.13	0.98	2.16
6	CH	CH	H	H	H	Cl	1.98	1.08	2.57
7	CH	CH	H	Cl	H	Cl	2.61	-1.00	2.81
8	CH	CH	H	H	H	Br	2.02	0.85	2.12
9	CH	CH	OMe	H	H	H	1.09	0.30	1.11
10	CH	CH	H	H	H	OMe	2.01	0.34	1.93
11	CH	CH	CN	H	H	H	1.63	1.31	2.02
12	CH	CH	H	CN	H	H	0.01	0.99	1.04
13	CH	CH	H	H	CN	H	2.16	0.77	2.86
14	CH	CH	H	H	H	CN	0.18	0.15	2.19
15	N	CH	H	H	H	H	2.07	0.45	3.44
16	CH	N	H	H	H	H	1.61	----	1.18
17	N	CH	H	H	H	F	0.85	-1.00	1.89
18	CH	C-F	H	H	H	F	1.05	0.18	3.03

* Molecule 16 has a fluorine atom bonded to C9 and an oxygen atom instead S1 (see skeleton numbering below).

Figures 2, 3 and 4 show graphical representations of the experimental date analyzed here.

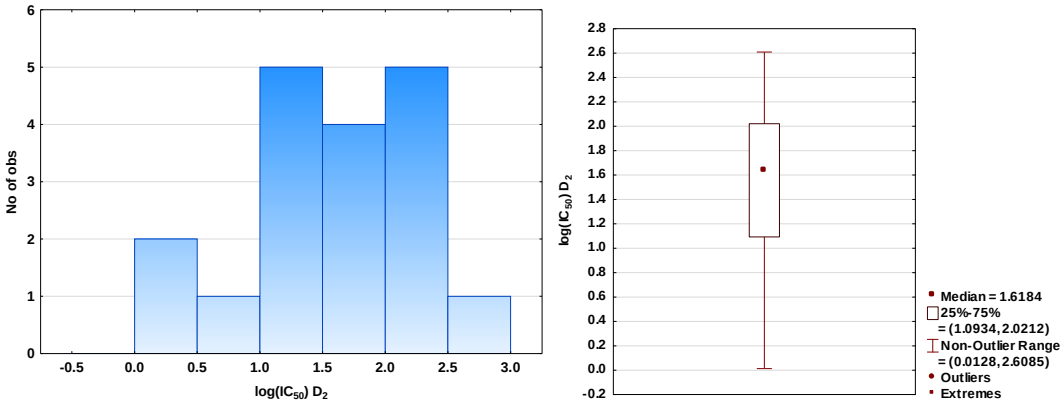

Figure 2: D_2 data: histogram of frequencies (left) and Box-Whiskers plot with median and quartile values (right)

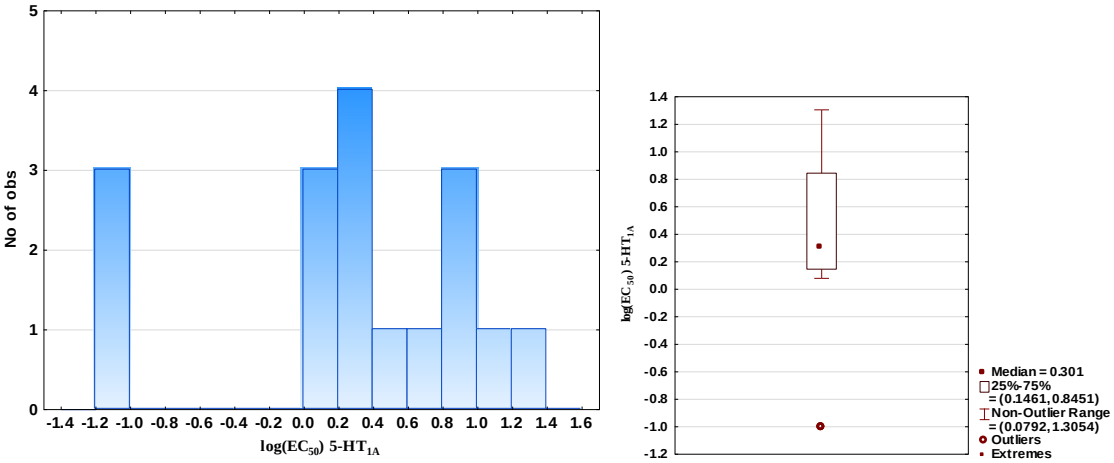

Figure 3: 5-HT_{1A} data: histogram of frequencies (left) and Box-Whiskers plot with median and quartile values (right)

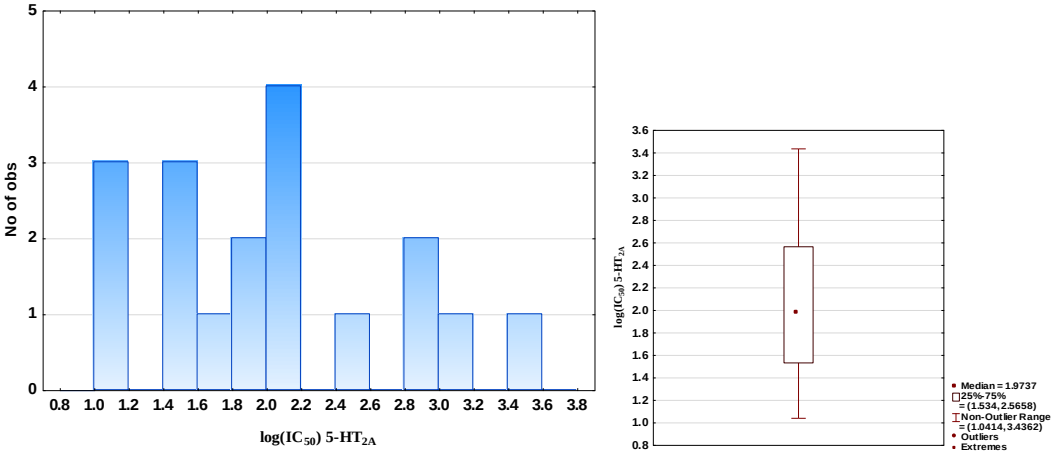

Figure 4: 5-HT_{2A} data: histogram of frequencies (left) and Box-Whiskers plot with median and quartile values (right)

Model and Calculations

This study employed the Klopman-Peradejordi-Gómez (KPG) method to obtain formal relationships between electronic structure and activity (FQSAR). It is based on the following master equation [26-39]:

$$\log(BA)=a+b\log\left(M_D\right)+\sum_{o=1}^{sub}\varphi_o+\sum_{i=1}^{Y}\left[e_iQ_i+f_iS_i^E+s_iS_i^N\right]+$$
$$+\sum_{i=1}^{Y}\sum_{m=(HOMO-2)^*,i}^{(HOMO)^*,i}\left[h_i\left(m\right)F_i(m^*)+j_i\left(m\right)S_i^E\left(m^*\right)\right]+$$
$$+\sum_{i=1}^{Y}\sum_{m'=(LUMO)^*,i}^{(LUMO+2)^*,i}\left[r_i\left(m'\right)F_i(m'^*)+t_i\left(m'\right)S_i^N\left(m'^*\right)\right]+$$
$$+\sum_{i=1}^{Y}\left[g_i\mu_i^*+k_i\eta_i^*+o_i\omega_i^*+z_i\zeta_i^*+w_jQ_i^{*,max}\right] \quad (1)$$

where BA is a biological activity (measured *in vivo* or *in vitro*), M_D is the drug's mass and φ_o is the orientational parameter of the o-th substituent (the summation on o runs over all the substituents selected for a particular research). Q_i is the net charge of atom i and S_i^E and S_i^N are, respectively, the total atomic electrophilic and nucleophilic superdelocalizabilities of atom i. F_{i,m^*} is the electron population of atom i in occupied (empty) local MO m* (m'*), $S_i^E(m)^*$ is the orbital electrophilic superdelocalizability at occupied local MO m* of atom i and $S_i^N(m')^*$ is the orbital nucleophilic superdelocalizability at empty local MO m'* of atom i. μ_i^*, η_i^*, ω_i^*, ζ_i^* and $Q_i^{*,max}$ are, respectively, the local atomic electronic chemical potential, the local atomic hardness, the local atomic electrophilicity, the local atomic softness and the maximal amount of electronic charge that atom i may accept. These indices were developed within the Hartree-Fock formalism and they are not the same than the ones developed within DFT [33]. The molecular orbitals with an asterisk correspond to the Local Molecular Orbitals (LMO) of each atom. For atom x, the LMOs are defined as the subset of the molecule's MOs having an electron population greater than 0.01e on x. In this study we have considered the three highest occupied local MOs ((HOMO)*, (HOMO-1)* and (HOMO-2)*) and the three lowest empty local MOs ((LUMO)*, (LUMO+1)* and (LUMO+2)*) of each atom because experimental evidence indicates that they could be determinant for molecular reactivity. The index Y runs over all atoms composing the molecule.

Good and very good results were obtained for different molecular systems and biological activities [13, 35, 40-63]. The coefficients accompanying each term in Eq. 1 must now be determined. This requires that a system of linear equations be constructed which must have the same number of terms for each molecule (i.e., the value of Y in Eq. 1 must be the same for all molecules). Since this usually does not happen, we must introduce the concept of a common skeleton. This common skeleton is defined as a certain set of atoms, common to all the molecules, which is expected to contain most of the information related to the biological activity. The common skeleton should be as inclusive as possible. For this case, the common skeleton is shown in Fig. 5.

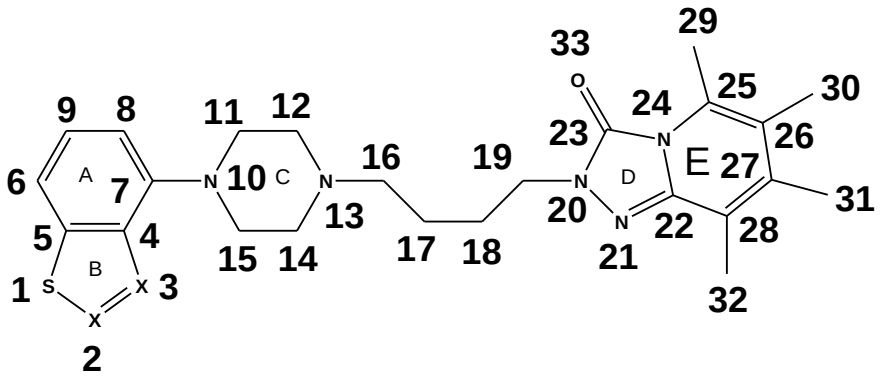

Figure 5: Common skeleton numbering

Note that this particular skeleton has 33 atoms and that each atom is described by 20 reactivity indices. This shows that Eq. 1 has at least 660 terms (plus the molecular mass and possibly the orientational effects). The way to deal with this fact is explained below.

The electronic structure of all molecules was calculated with the Density Functional Theory (DFT) at the B3LYP/6-31g(d,p) level after full geometry optimization. The Gaussian suite of programs was used [64]. All the information to calculate the numerical values for the local atomic reactivity indices was obtained from the Gaussian results with the D-Cent-QSAR software [65]. All the electron populations smaller than or equal to 0.01 e were considered as zero [33]. Negative electron populations coming from Mulliken Population Analysis were corrected as usual [66]. Because the resolution of the system of linear equations 1 is not possible because we have not enough molecules, we used Linear Multiple Regression Analysis (LMRA) techniques to find the best possible solution. For each case, a matrix containing the dependent variable (the biological activity) and the local atomic reactivity indices of all atoms of the common skeleton as independent variables was built. The Statistica software was used for LMRA [67].

Results

Results for the activity at the 5-HT$_{1A}$ receptor

The best equation found is:

$$\log(\mathrm{EC}_{50}) = -37.67 - 0.57\mathbf{S}_{27}^{\mathbf{E}}(\mathbf{HOMO}-\mathbf{2})^{*} + 3.17\boldsymbol{\eta}_{\mathbf{19}} + \\ +4.61\mathbf{F}_{\mathbf{20}}(\mathbf{LUMO}+\mathbf{1})^{*} - 1.64\mathbf{Q}_{\mathbf{26}} + 0.30\mathbf{S}_{\mathbf{12}}^{\mathbf{N}} \quad (2)$$

with n=17, R= 0.98, R^2= 0.96, adjusted R^2= 0.94, F(5,11)=55.294 ($p<0.00000$) and a standard error of estimate of 0.17. No outliers were detected and no residuals fall outside the $\pm 2\sigma$ limits. Here, S_{27}^{E}(HOMO-2)* is the electrophilic superdelocalizability of the third highest occupied local MO of atom 27, η_{19} is the local atomic hardness of atom 19, F_{20}(LUMO+1)* is the Fukui index of the second lowest empty local MO of atom 20, Q_{26} is the net charge of atom 26 and S_{12}^{N} is the total atomic nucleophilic superdelocalizability of atom 12. Tables 2 and 3 show the beta coefficients, the results of the t-test for significance of coefficients and the matrix of squared correlation coefficients for the variables of Eq. 2. There are no significant internal correlations between independent variables (Table 3). Figure 6 displays the plot of observed *vs.* calculated log(EC_{50}).

Table 2: Beta coefficients and t-test for significance of coefficients in Eq. 2

Var.	Beta	t(11)	p-level
$\mathbf{S_{27}^{E}(HOMO-2)^{*}}$	-0.52	-7.38	0.00001
$\boldsymbol{\eta_{19}}$	0.27	4.40	0.001
$\mathbf{F_{20}(LUMO+1)^{*}}$	0.59	8.85	0.000002
$\mathbf{Q_{26}}$	-0.34	-5.28	0.0002
$\mathbf{S_{12}^{N}}$	0.33	5.41	0.0002

Table 3: Matrix of squared correlation coefficients for the variables in Eq. 2

	S_{27}^{E}(HOMO-2)*	η_{19}	F_{20}(LUMO+1)*	Q_{26}	S_{12}^{N}
S_{27}^{E}(HOMO-2)*	1.00				
η_{19}	0.06	1.00			
F_{20}(LUMO+1)*	0.17	0.02	1.00		
Q_{26}	0.08	0.00	0.01	1.00	
S_{12}^{N}	0.03	0.03	0.01	0.01	1.00

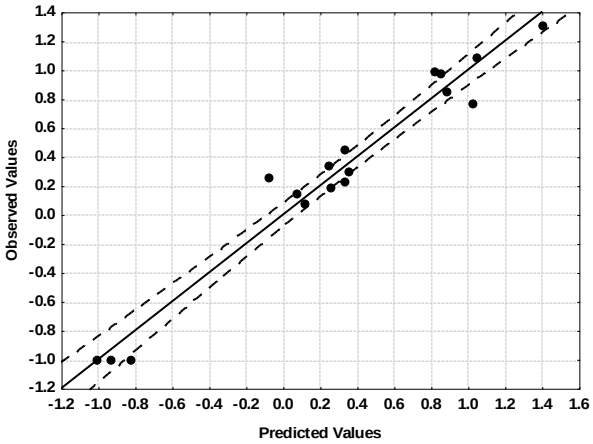

Figure 6: Plot of predicted vs. observed log(EC_{50}) values (Eq. 2). Dashed lines denote the 95% confidence interval

The associated statistical parameters of Eq. 2 indicate that this equation is statistically significant and that the variation of the numerical values of a group of five local atomic reactivity indices of atoms belonging to the common skeleton explains about 96% of the variation of log(EC_{50}). Figure 6, spanning about 1.4 orders of magnitude, shows that there is a relatively good correlation of observed *versus* calculated values. Figures 7, 8 and 9 show, respectively, the plot of predicted values *vs.* residuals scores, the plot of residual *vs.* deleted residuals and the normal probability plot of residuals. These figures give support to the hypothesis that the linear form of Eq. 1 is a good first approach to be employed in this case. Let us notice that Eq. 1 is a truncated form of a longer equation containing non-linear terms (quadratic, cubic, etc.) of the local atomic reactivity indices.

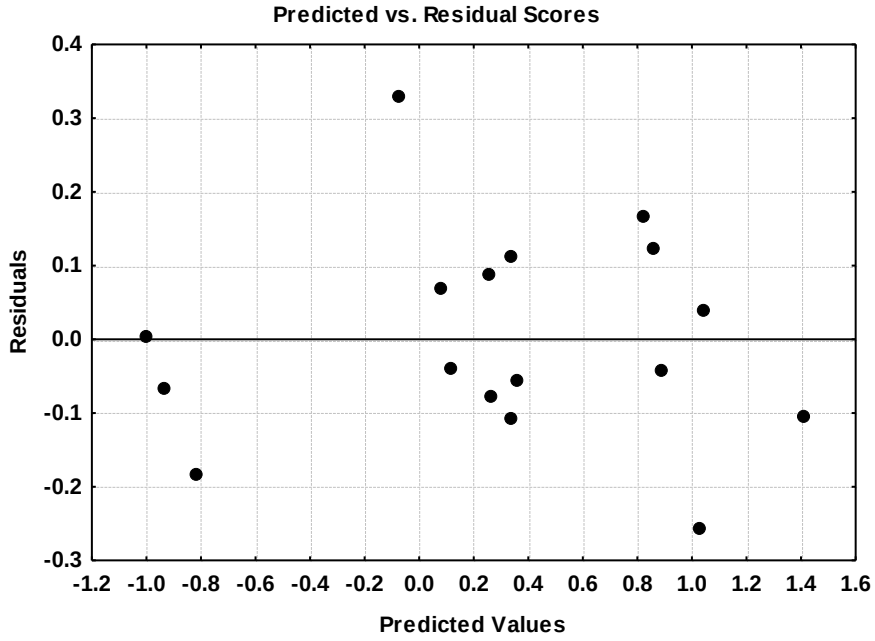

Figure 7: Plot of predicted values vs. residuals scores

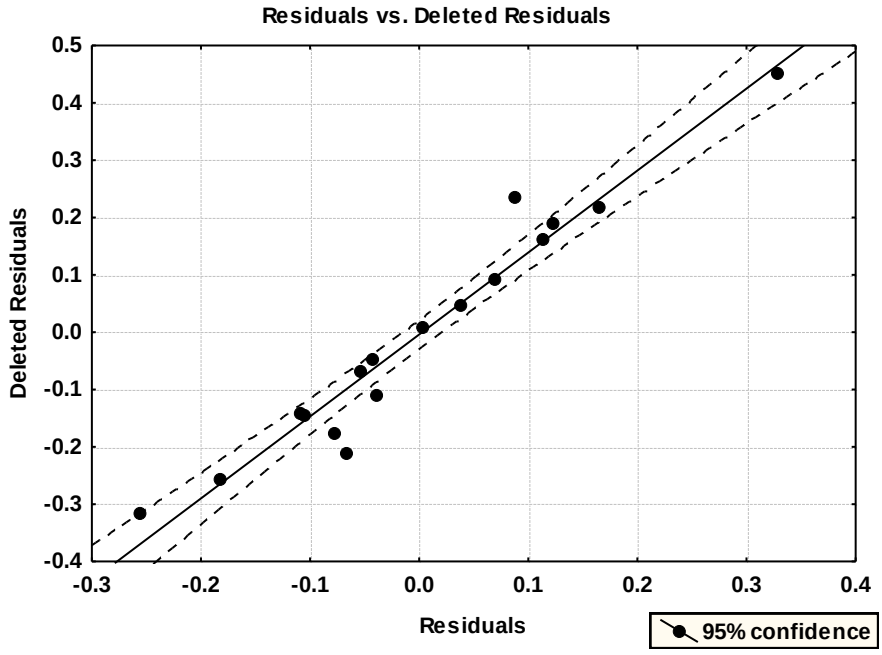

Figure 8: Plot of residuals vs. deleted residuals

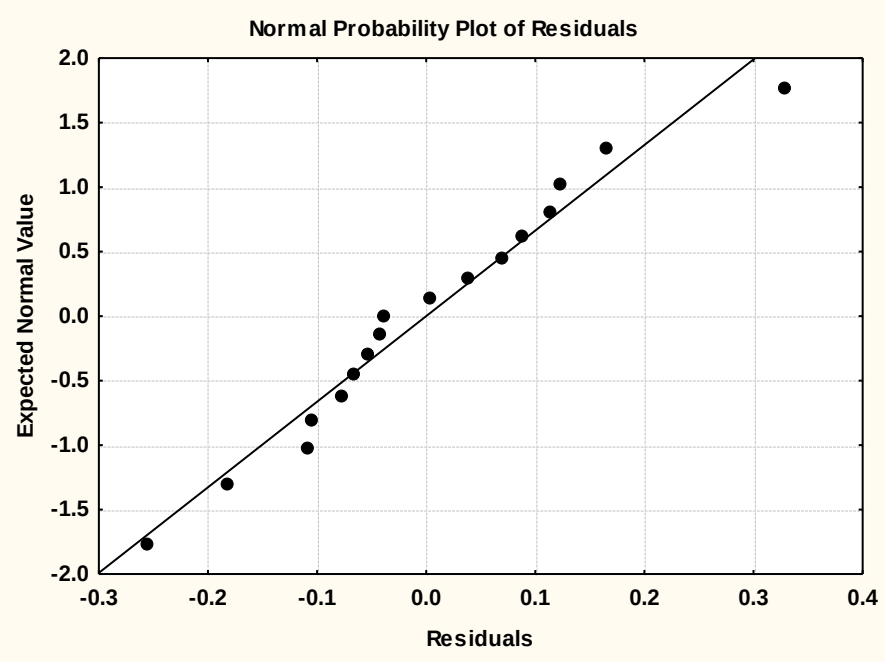

Figure 9: Normal probability plot of residuals

Results for the activity at the 5-HT$_{2A}$ receptor

The best equation found is:

$$\log(IC_{50}) = -88.11 + 4.66S_{13}^{N} - 3.24S_{18}^{E}(HOMO-1)^{*} + 0.04S_{2}^{N}(LUMO+1)^{*} - \\ -3.16S_{11}^{N}(LUMO+2)^{*} + 0.59S_{20}^{E}(HOMO-2)^{*} - 0.003S_{30}^{N}(LUMO)^{*} \quad (3)$$

with n=18, R=0.98, R²=0.96, adjusted R²=0.93, F(6,11)=39.523 (p<0.00001) and a standard error of estimate of 0.18. No outliers were detected and no residuals fall outside the ±2σ limits. Here, S_{13}^{N} is the total atomic nucleophilic superdelocalizability of atom 13, S_{18}^{E}(HOMO-1)* is the electrophilic superdelocalizability of the second highest occupied local MO of atom 18, S_{2}^{N}(LUMO+1)* is the nucleophilic superdelocalizability of the second lowest empty MO of atom 2, S_{11}^{N}(LUMO+2)* is the nucleophilic superdelocalizability of the third lowest empty MO of atom 11, S_{20}^{E}(HOMO-2)* is the electrophilic superdelocalizability of the third highest occupied local MO of atom 20 and S_{30}^{N}(LUMO)* is the nucleophilic superdelocalizability of the lowest empty MO of atom 30. Tables 4 and 5 show the beta coefficients, the results of the t-test for significance of coefficients and the matrix of squared correlation coefficients for the variables of Eq. 3. There are no significant internal correlations between independent variables (Table 5). Figure 10 displays the plot of observed *vs.* calculated log(IC_{50})

Table 4: Beta coefficients and t-test for significance of coefficients in Eq. 3

Var.	Beta	t(11)	p-level
S_{13}^{N}	0.86	12.38	0.000000
S_{18}^{E}(HOMO-1)*	-0.54	-7.76	0.000009
S_{2}^{N}(LUMO+1)*	0.38	5.54	0.0002
S_{11}^{N}(LUMO+2)*	-0.36	-5.46	0.0002
S_{20}^{E}(HOMO-2)*	0.38	5.34	0.0002
S_{30}^{N}(LUMO)*	-0.26	-3.62	0.004

Table 5: Matrix of squared correlation coefficients for the variables in Eq. 3

	S_{13}^{N}	S_{18}^{E}(HOMO-1)*	S_{2}^{N}(LUMO+1)*	S_{11}^{N}(LUMO+2)*	S_{20}^{E}(HOMO-2)*
S_{18}^{E}(HOMO-1)*	0.08	1.00			

S_2^N(LUMO+1)*	0.01	0.04	1.00		
S_{11}^N(LUMO+2)*	0.00	0.02	0.04	1.00	
S_{20}^E(HOMO-2)*	0.00	0.01	0.04	0.04	1.00
S_{30}^N(LUMO)*	0.05	0.00	0.00	0.02	0.15

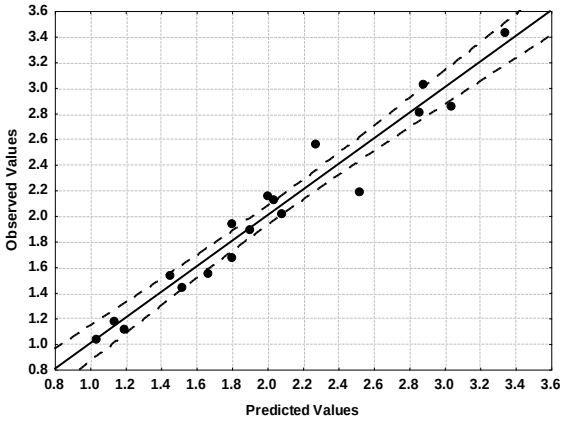

Figure 10: Plot of predicted vs. observed log(IC_{50}) values (Eq. 3). Dashed lines denote the 95% confidence interval

The associated statistical parameters of Eq. 3 indicate that this equation is statistically significant and that the variation of the numerical values of a group of six local atomic reactivity indices of atoms belonging to the common skeleton explains about 93% of the variation of log(IC_{50}). Figure 10, spanning about 2 orders of magnitude, shows that there is a relatively good correlation of observed *versus* calculated values. Figures 11, 12 and 13 show, respectively, the plot of predicted values *vs.* residuals scores, the plot of residual *vs.* deleted residuals and the normal probability plot of residuals. The figures support the hypothesis that the linear form of Eq. 1 is a good approach to be employed in this case.

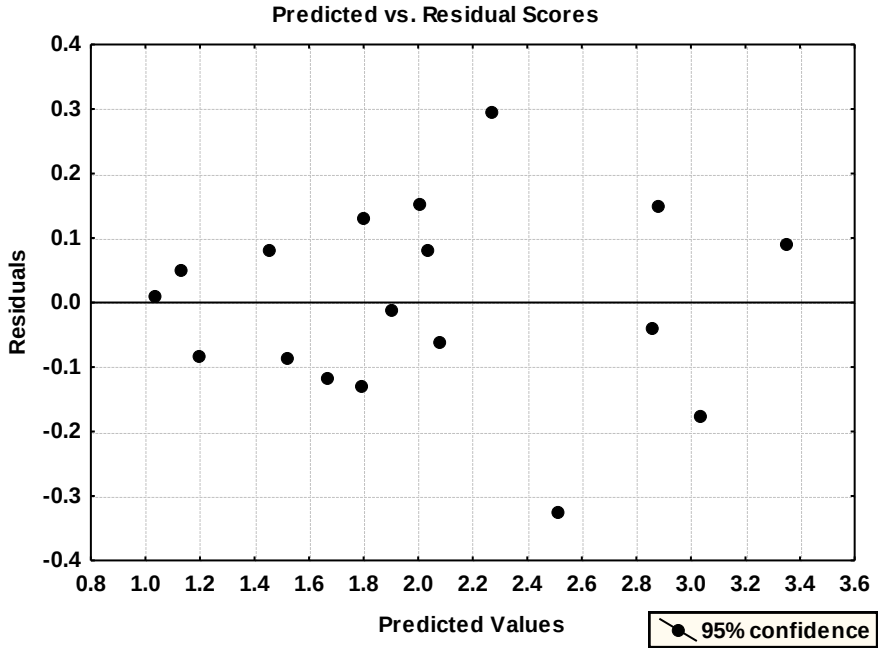

Figure 11: Plot of predicted values vs. residuals scores

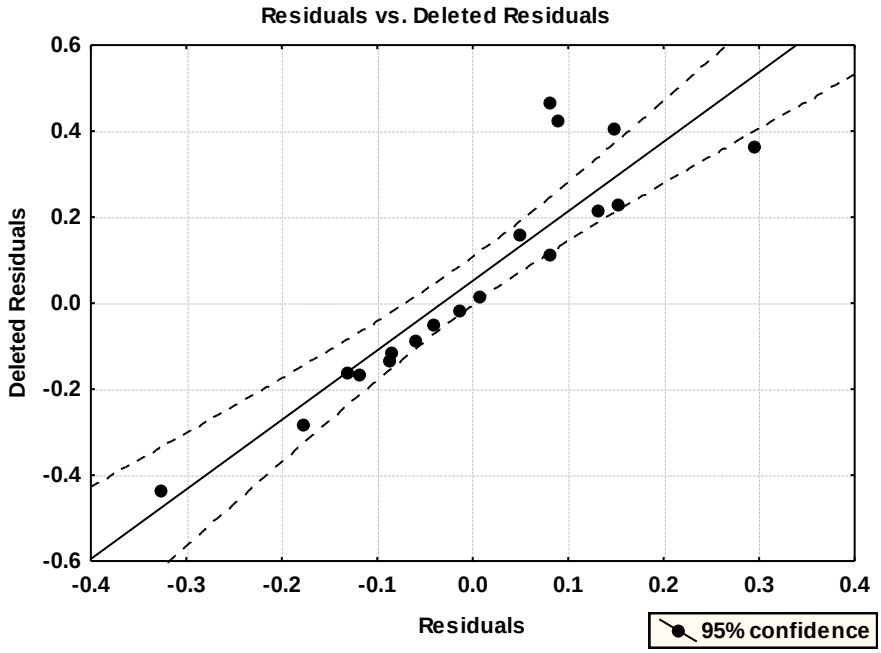

Figure 12: Plot of residuals vs. deleted residuals

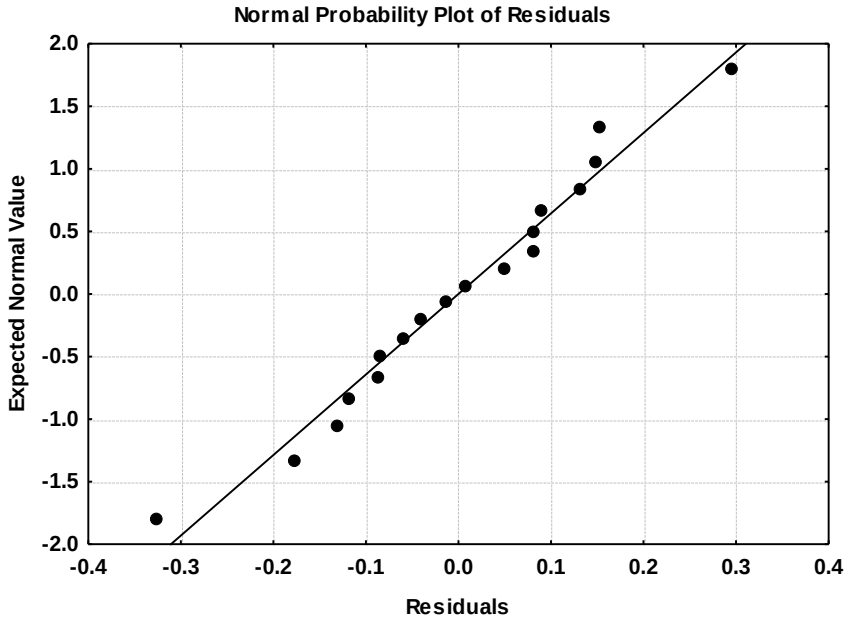

Figure 13: Normal probability plot of residuals

Results for D_2

The best equation found is:

$$\log\left(\mathrm{IC}_{50}\right) = 11.43 + 1.88\boldsymbol{\omega}_{31} + 2.69\mathbf{S}_{30}{}^{\mathbf{E}}\left(\mathbf{HOMO}\right)^{*} - 0.35\mathbf{S}_{8}{}^{\mathbf{N}}\left(\mathbf{LUMO}+\mathbf{2}\right)^{*} + \\ +2.32\mathbf{F}_{31}\left(\mathbf{LUMO}\right)^{*} - 0.40\mathbf{S}_{18}{}^{\mathbf{N}} - 0.91\mathbf{Q}_{26} \qquad (4)$$

with n=18, R=0.98, R^2=0.96, adjusted R^2=0.93, F(6,11)=39.869 ($p<0.00000$) and a standard error of estimate of 0.18. No outliers were detected and no residuals fall outside the $\pm 2\sigma$ limits. Here, ω_{31} is the local atomic electrophilicity of atom 31, $S_{30}{}^{E}$(HOMO)* is the electrophilic superdelocalizability of the highest occupied local MO

of atom 30, S_8^N(LUMO+2)* is the nucleophilic superdelocalizability of the third lowest empty local MO of atom 8, F_{31}(LUMO)* is the Fukui index of the highest occupied local MO of atom 31, S_{18}^N is the total atomic nucleophilic superdelocalizability of atom 18 and Q_{26} is the net charge of atom 26. Tables 6 and 7 show the beta coefficients, the results of the t-test for significance of coefficients and the matrix of squared correlation coefficients for the variables of Eq. 4. There are no significant internal correlations between independent variables (Table 7). Figure 14 displays the plot of observed *vs.* calculated log(IC_{50}) values.

Table 6: Beta coefficients and t-test for significance of coefficients in Eq. 4

Var.	Beta	t(11)	p-level
ω_{31}	0.94	13.26	0.000000
S_{30}^E(HOMO)*	0.44	6.48	0.00005
S_8^N(LUMO+2)*	-0.42	-6.51	0.00004
F_{31}(LUMO)*	0.38	5.34	0.0002
S_{18}^N	-0.22	-3.46	0.005
Q_{26}	-0.19	-2.94	0.01

Table 7: Matrix of squared correlation coefficients for the variables in Eq. 4

	ω_{31}	S_{30}^E(HOMO)*	S_8^N(LUMO+2)*	F_{31}(LUMO)*	S_{18}^N
ω_{31}	1.00				
S_{30}^E(HOMO)*	0.06	1.00			
S_8^N(LUMO+2)*	0.05	0.02	1.00		
F_{31}(LUMO)*	0.14	0.12	0.01	1.00	
S_{18}^N	0.00	0.01	0.00	0.00	1.00
Q_{26}	0.00	0.00	0.00	0.00	0.01

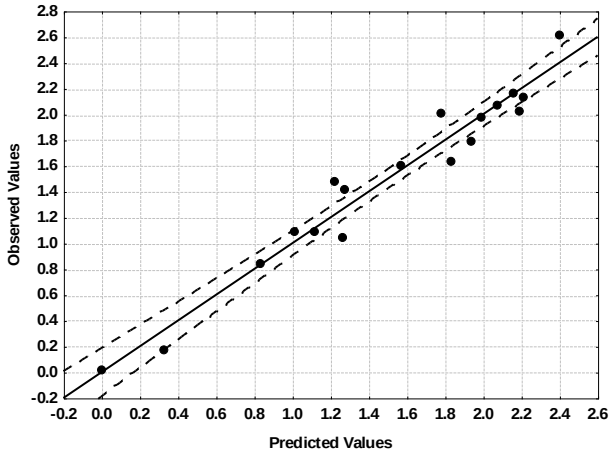

Figure 14: Plot of predicted vs. observed log(IC_{50}) values (Eq. 4). Dashed lines denote the 95% confidence interval

The associated statistical parameters of Eq. 4 indicate that this equation is statistically significant and that the variation of the numerical values of a group of six local atomic reactivity indices of atoms belonging to the common skeleton explains about 93% of the variation of log(IC_{50}). Figure 14, spanning about 2.4 orders of magnitude, shows that there is a relatively good correlation of observed *versus* calculated values. Figures 15, 16 and 17 show, respectively, the plot of predicted values vs. residuals scores, the plot of residual vs. deleted residuals and the normal probability plot of residuals. The figures back the hypothesis that the linear form of Eq. 1 is an acceptable method to be employed in this case.

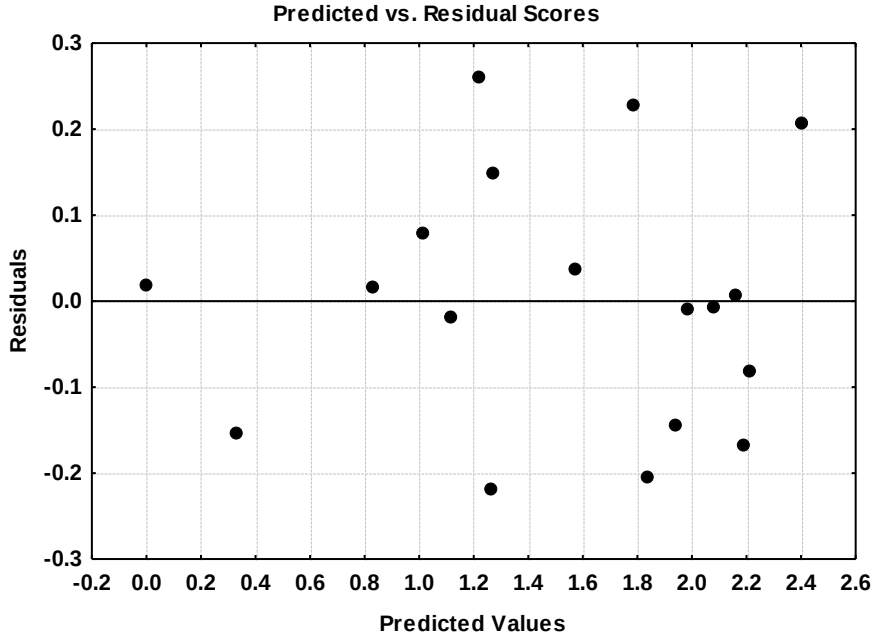

Figure 15: Plot of predicted values vs. residuals scores

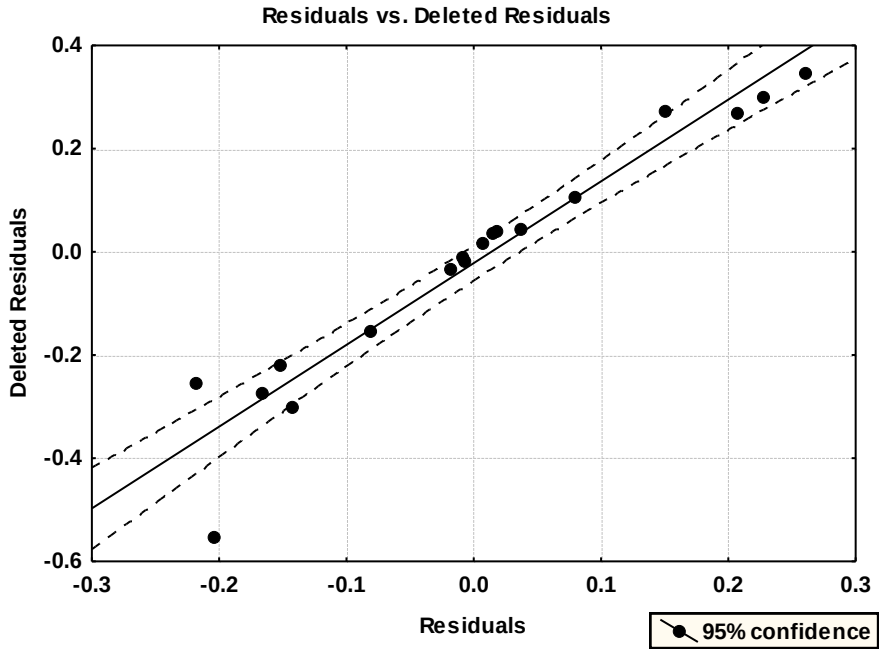

Figure 16: Plot of residuals vs. deleted residuals

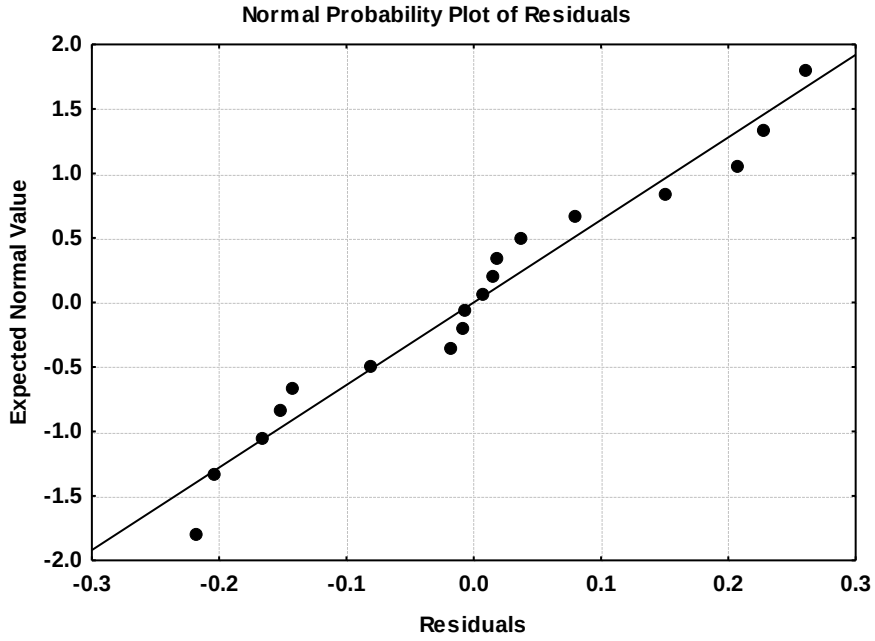

Figure 17: Normal probability plot of residuals

Local Molecular Orbitals

If a local atomic reactivity index of an inner occupied local MO (i.e., (HOMO-1)* and/or (HOMO-2)*) or of a higher vacant local MO ((LUMO+1)* and/or (LUMO+2)*) appears inside an equation, this means that the remaining of the upper occupied MOs (for example, if (HOMO-2)* appears, upper means (HOMO-1)* and (HOMO)*) or the remaining of the empty MOs (for example, if (LUMO+1)* appears, lower means the (LUMO)*) also contribute to the interaction. Their absence in the equation only means that the variation of their numerical values does not account for the variation of the numerical value of the biological property. We work with the hypothesis that any algebraic conditions imposed on the numerical values of a local atomic reactivity index belonging to an inner occupied local MO or to an upper empty local MO of a given atom also hold for the corresponding local MOs having a lower energy. Tables 8 to 10 show the local MO structure of atoms appearing in Eq. 2 to 4 Nomenclature: Molecule (HOMO) / (HOMO-2)* (HOMO-1)* (HOMO)* - (LUMO)* (LUMO+1)* (LUMO+2).

Table 8: Local Molecular Orbitals of atoms 2, 8, 11 and 12

Mol.	Atom 2	Atom 8	Atom 11 (σ)	Atom 12 (σ)
1 (108)	105π106π108π- 110π113σ114π	105π106π108π- 110π111π114π	105σ106σ108σ- 111σ118σ122σ	105σ106σ108σ- 120σ122σ124σ
2 (112)	109π110π112π- 114π117σ118π	109π110π112π- 114π115π118π	109σ110σ112σ- 115σ123σ126σ	109σ110σ112σ- 124σ125σ126σ
3 (112)	109π110π112π- 114π117σ119π	109π110π112π- 114π115π119π	109σ110σ112σ- 115σ123σ126σ	109σ110σ112σ- 124σ125σ126σ
4 (116)	113π114π116π- 118π122π123π	113π114π116π- 118π120π123π	113σ114σ116σ- 120σ128σ131σ	113σ114σ116σ- 129σ130σ131σ
5 (116)	113π114π116π- 118π121σ123π	113π114π116π- 118π119π123π	113σ114σ116σ- 119σ127σ130σ	113σ114σ116σ- 128σ130σ133σ
6 (116)	113π114π116π- 118π121σ123π	113π114π116π- 118π119π123π	113σ114σ116σ- 119σ127σ130σ	113σ114σ116σ- 128σ129σ130σ
7 (124)	121π 122π124π -126π 130σ132	121π122π124π– 126π 128π132π	121σ122σ124σ- 128σ136σ139σ	121σ122σ124σ- 137σ138σ139σ

	π			
8 (125)	122π123π125π-127π131σ132π	122π123π125π-127π128π132π	122σ123σ125σ-128σ136σ140σ	122σ123σ125σ-137σ138σ139σ
9 (116)	113π114π116π-118π121σ 122π	113π114π116π-118π119π122π	113σ114σ116σ-119σ127σ131σ	113σ114σ116σ-129σ131σ132σ
10 (116)	113π114π116π-118π121σ122π	113π114π116π-118π119π122π	113σ114σ116σ-119σ127σ131σ	113σ114σ116σ-129σ131σ133σ
11 (116)	113π114π116π-118π121σ 122π	113π114π116π-118π119π122π	113σ114σ116σ-119σ124σ126σ	126σ127σ128σ
12 (116)	113π114π116π-118π121σ 122π	113π114π116π-118π119π122π	113σ114σ116σ-119σ127σ131σ	113σ114σ116σ-128σ131σ133σ
13 (116)	113π114π116 π- 118π121σ 122π	113π114π116 π-118π119π122 π	113σ114σ116σ-119σ127σ130σ	113σ114σ116σ-128σ131σ133σ
14 (116)	113π114π116π-118π121σ 122π	113π114π116π-118 π119π122π	113σ114σ116σ-119σ127σ131σ	113σ114σ116σ-129σ131σ132σ
15 (108)	105π106π108π-110π 111π 113σ	105π106π108π-111π114π123σ	105σ106σ108σ-111σ119σ120σ	98σ106σ108σ-117σ118σ121σ
16 (108)	102π105π106π-110π111π113π	102σ105π106π-110π111π113π	100σ102σ107σ-123σ126σ128σ	100σ102σ107σ-118σ119σ124σ
17 (112)	109π110π112π-114π115σ 117σ	109π110π112π-115π116π118π	109σ110σ112σ-115σ124σ126σ	103σ110σ112σ-122σ123σ126σ
18 (116)	113π114π116π-118π121σ122π	113π114π116π-118π119π123π	109σ114σ116σ-119σ127σ131σ	112σ114σ116σ-128σ130σ131σ

Table 9: Local Molecular Orbitals of atoms 18, 19, 20 and 26

Mol.	Atom 18 (σ)	Atom 19 (σ)	Atom 20	Atom 26
1 (108)	100σ102σ107σ-117σ121σ122σ	100σ102σ103σ-115σ119σ121σ	102σ103π107π-109π115π117σ	100π102σ107π-109π112π124π
2 (112)	104σ106σ111σ-122σ126σ127σ	104σ106σ107σ-119σ120σ125σ	106σ107π111π-113π119π120π	104π106σ111π-113π116π119π
3 (112)	106σ107σ111σ-122σ126σ128σ	104σ106σ107σ-120σ125σ127σ	106σ107π111π-113π118π120π	104π106σ111π-113π116π118π
4 (116)	109σ111σ115σ-127σ130σ131σ	108σ109σ111σ-124σ130σ131σ	109σ111π115π-117π124σ125π	108π109π 115π-117π119π121π
5 (116)	108σ110σ115σ-126σ130σ131σ	107σ110σ111σ-124σ129σ130σ	110σ111π115π-117π124π128σ	108π110σ115π-117π120π122σ
6 (116)	108σ110σ115σ-126σ130σ131σ	108σ110σ111σ-124σ129σ131σ	110σ111π115π-117π124π128σ	108π110σ115π-117π120π122π
7 (124)	118σ119σ123σ-135σ138σ139σ	115σ118σ119σ-133σ138σ139σ	118σ 119π123π-125π131σ133π	118σ119π123π-125π127π 129π
8 (125)	119σ120σ124σ-135σ139σ140σ	117σ119σ120σ-133σ138σ140σ	119σ120π124π-126π133π137σ	117π120π124π-126π129π130π
9 (116)	110σ111σ115σ-	108σ110σ111σ-	110σ111π115π-	110σ111π115π-

	125σ132σ133σ	123σ128σ130σ	117π123π125σ	117π120π126σ
10 (116)	107σ108σ111σ- 125σ130σ131σ	108σ110σ111σ- 123σ126σ130σ	110σ111π115π- 117π123π125σ	108π111π115π- 117π120π128π
11 (116)	109σ110σ115σ- 126σ129σ133σ	107σ109σ110σ- 123σ127σ129σ	110π111σ115π- 117π123π126σ	110π111σ115π- 117π120π124π
12 (116)	107σ109σ115σ- 125σ130σ131σ	106σ109σ110σ- 123σ129σ130σ	109σ110π115π- 117π123π128σ	109σ111π115π- 117π120π126π
13 (116)	107σ109σ115σ- 125σ130σ132σ	106σ109σ110σ- 123σ129σ131σ	110π111σ115π- 117π123π125σ	107π109σ115π- 117π120π132π
14 (116)	107σ109σ115σ- 125σ130σ131σ	107σ109σ110σ- 123σ128σ130σ	109σ110π115π- 117π123π125σ	107π109σ115π- 117π120π126σ
15 (108)	99σ101σ107σ- 117σ121σ122σ	99σ101σ102σ- 115σ120σ122σ	101σ102σ107π- 109π115π120σ	99π101π107π- 109π112π122π
16 (108)	104σ107σ108σ- 121σ122σ123σ	101σ103σ104σ- 114σ119σ120σ	103σ104π108π- 109π114π115π	101π103σ108π- 109π112π122σ
17 (112)	103σ105σ111σ- 122σ126σ127σ	103σ105σ106σ- 120σ124σ125σ	105σ106σ111π- 113π119π120π	103π105π111π- 113π115π116π
18 (116)	110σ111σ115σ- 126σ131σ133σ	108σ110σ111σ- 125σ129σ132σ	110σ111π115π- 117π124π125σ	108π110σ115π- 117π120π124σ

Table 10: Local Molecular Orbitals of atoms 27, 30 and 31

Mol.	**Atom 27**	**Atom 30**	**Atom 31**
1 (108)	99π100π107π- 109π112π115π	83σ84σ85σ- 118σ119σ120σ	83σ84σ85σ- 118σ119σ121σ
2 (112)	104π106σ111π- 113π116π119π	104π106π111π- 116π119π129π	84σ89σ90σ- 119σ124σ125σ
3 (112)	103π104π111π- 113π116π118π	80σ81σ89σ- 118σ124σ125σ	81σ83σ89σ- 118σ124σ125σ
4 (116)	107π108π115π- 117π119π121π	108π109π115π- 119π121σ125σ	87σ88σ89σ- 121σ132σ135σ
5 (116)	108π110σ115π- 117π120π122π	108π110σ115π- 120lp122σ131σ	86σ87σ88σ- 122σ128σ129σ
6 (116)	108π110σ115π- 117π120π122π	85σ86σ87σ- 122σ128σ129σ	86σ87σ88σ- 122σ128σ129σ
7 (124)	113σ116π123π- 125π127π129π	118σ119π123π- 127π129σ131σ	91σ93σ94σ- 129σ138σ139σ
8 (125)	117π120π124π- 126π129π130π	95σ96σ99σ- 129σ137σ138σ	96σ98σ99σ- 129σ137σ138σ
9 (116)	108π110σ115π- 117π120π123π	89σ90σ91σ- 126σ127σ128σ	89σ90σ100σ- 126σ127σ128σ
10 (116)	108π111π115π- 117π120π123π	84σ 85σ101σ- 126σ128σ130σ	85σ89σ90σ- 126σ127σ128σ
11 (116)	107π111σ115π- 117π120π123π	89σ 90σ 91σ- 127σ128σ129σ	91σ94σ96σ- 127σ128σ129σ
12 (116)	107π109σ115π- 117π120π123π	114π115π116π- 117π119π120π	88σ92σ94σ- 126σ127σ128σ
13 (116)	107π111π115π-	85σ 86σ 91σ-	97σ107π111π-

	117π120π123π	126σ127σ129σ	117π126σ129σ
14 (116)	106π107π115π-	88σ89σ92σ-	88σ89σ94σ-
	117π120π123π	128σ129σ130σ	126σ128σ130σ
15 (108)	98π99π107π-	81σ83σ84σ-	83σ85σ86σ-
	109π112π115π	118σ119σ121σ	118σ119σ120σ
16 (108)	101π102π108π-	82σ84σ86σ-	84σ85σ86σ-
	109π112π115π	117σ118σ119σ	117σ118σ119σ
17 (112)	102π103π111π-	80σ88σ89σ-	85σ88σ89σ-
	113π116π119π	119σ123σ124σ	119σ123σ124σ
18 (116)	107π108π115π-	84σ85σ93σ-	87σ88σ93σ-
	117π120π124π	124σ128σ129σ	124σ128σ129σ

Discussion

Discussion of the activity at the 5-HT_{1A} receptor

Table 2 shows that the importance of variables in Eq. 2 is F_{20}(LUMO+1)*> S_{27}^{E}(HOMO-2)*>> Q_{26}> S_{12}^{N}> η_{19}. A high activity at the 5-HT_{1A} receptor is associated with small numerical values for S_{27}^{E}(HOMO-2)*, η_{19} and F_{20}(LUMO+1)*, a positive net charge on atom 26 and with small numerical values for S_{12}^{N}.

Atom 27 is an aromatic carbon atom in ring D (Fig. 5). Table 10 shows that $(HOMO)_{27}^{*}$ coincides with the molecular HOMO or (HOMO-1). $(LUMO)_{27}^{*}$ coincides with the molecular LUMO. A high activity is associated with small numerical values for S_{27}^{E}(HOMO-2)*. These small values are obtained by shifting downwards the MO energy and/or making zero the electron density of this MO on atom 27 (remember that S_{27}^{E}(HOMO-2)*= F_{27}(HOMO-2)*/$E_{(HOMO-2)*}$). Following our suggested interpretation, an optimal situation takes place when $(HOMO)_{27}^{*}$ coincides with an inner occupied MO of the molecule (i.e., its energy is very far from the molecular HOMO). Therefore, this atom should behave as a good electron acceptor and be interacting with an electron-rich π center such an anion (COO^{-} for example) or an aromatic system (π-anion or π-π interaction). Atom 19 is a sp^3 carbon in the chain linking rings C and D (Fig. 5). All local MOs have a sigma nature (Table 9). $(HOMO)_{19}^{*}$ y $(LUMO)_{19}^{*}$ do not coincide with the corresponding molecular HOMO and LUMO but with MOs being distant from them in the energy axis. A high activity is associated with small numerical values for η_{19} the local atomic hardness. This means that the resistance to exchange electrons with the environment is low. On this basis, and because C19 is a polarized atom adjacent to a nitrogen atom, the first option is a non-classical carbon hydrogen bond C19-H…X (X=O or N and with d=3-3.9Å). Also, alkyl (d=5-5.5Å) or alkyl-π (d=5-5.5Å) interactions are possible. Atom 20 is nitrogen in ring D (Fig. 5). A high activity is associated with small numerical values for F_{20}(LUMO+1)*. Table 9 shows that $(LUMO)_{20}^{*}$ has a π nature in all cases and that $(LUMO+1)_{20}^{*}$ has a π nature in all but one case. Small numerical values are obtained when diminishing the electronic density in this local MO. Therefore, the optimal situation should occur when $(LUMO)_{20}^{*}$ and $(LUMO+1)_{20}^{*}$ coincide with upper empty MOs of the molecule (see the case of atom 27). Atom 20 should behave then as a bad electron acceptor. Table 9 also shows that $(HOMO)_{20}^{*}$ coincides with the molecular HOMO or (HOMO-1). All these data suggest that atom N20 seems to be involved in a hydrogen bond of the N20…H-X. An additional possibility is a π-π interaction. Atom 26 is an aromatic carbon in ring D (Fig. 5). This atom should have a positive net charge for an improved activity. Therefore, it is possible that C26 be participating in an electrostatic interaction with a negatively charged center. It is interesting to note that C26 is bonded to C27 and that it was suggested above that C27 could also be interacting with an anion. Atom 12 is a sp^3 carbon in ring C (Fig. 5). All local MOs have a sigma nature (Table 8). A high activity at the 5-HT_{1A} receptor is associated with small numerical values for S_{12}^{N}. This means that atom 12 should be a bad electron acceptor, fact supported by the fact that $(LUMO)_{12}^{*}$ coincides with MOs that are very far from the molecular LUMO. Table 8 also shows that $(HOMO)_{12}^{*}$coincides with the molecular HOMO, suggesting that atom 12 is engaged in a weak hydrogen bond C12-H…X (X=O or N). In addition, alkyl or alkyl-π interactions are possible like in the case of atom 19. All the suggestions are displayed in the partial 2D pharmacophore of Fig. 18.

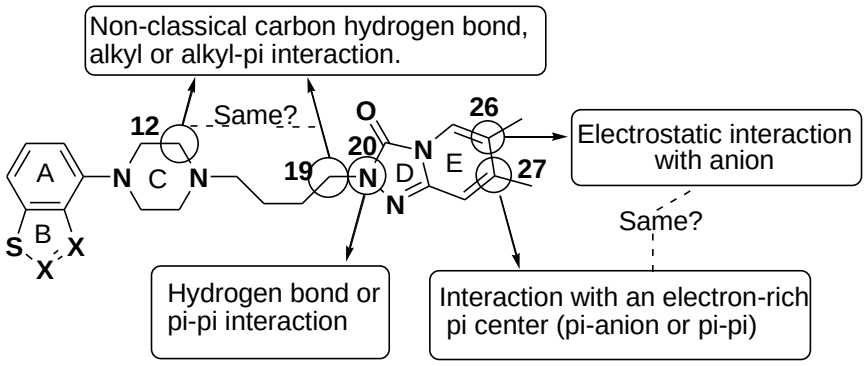

Figure 18: Partial 2D pharmacophore for activity at the 5-HT$_{1A}$ receptor

Discussion of the activity at the 5-HT$_{2A}$ receptor

Table 4 shows that the importance of variables in Eq. 3 is S_{13}^{N}>> S_{18}^{E}(HOMO-1)* >> S_{2}^{N}(LUMO+1)* = S_{20}^{E}(HOMO-2)* > S_{11}^{N}(LUMO+2)* > S_{30}^{N}(LUMO)*. A high activity at the 5-HT$_{2A}$ receptor is associated with small numerical values for S_{13}^{N}, S_{18}^{E}(HOMO-1)* and S_{2}^{N}(LUMO+1)*, large numerical values for S_{11}^{N}(LUMO+2)* and S_{30}^{N}(LUMO)* and large (negative) numerical values for S_{20}^{E}(HOMO-2)*.

Atom 13 is nitrogen in ring C (Fig. 5). A high activity is associated with small numerical values for S_{13}^{N}. Remembering that:

$$S_{13}^{N} = \sum_{r=1}^{\text{local MOs}} \frac{F_{13}(OM_r^*)}{E_r} \qquad (5)$$

We can see that the dominant terms are the lowest empty local MOs (because of their lower energy). Therefore, the only way to obtain small numerical values is by making $(HOMO)_{13}^{*}$ to coincide with an empty molecular MO having a higher energy that the LUMO. This makes atom 13 a bad electron acceptor. Therefore, we suggest that this atom is interacting with an electron-deficient center, perhaps through its lone pair. Atom 18 is a sp^3 carbon in the chain linking rings C and D (Fig. 5). Table 9 shows that all local MOs have a σ character, that the local $(HOMO)_{18}$* coincides with the molecular HOMO or (HOMO-1) and that the local $(LUMO)_{18}$* coincides with molecular empty MOs having a higher energy that the LUMO. A high activity is associated with small numerical values for S_{18}^{E}(HOMO-1)* and S_{18}^{E}(HOMO)* (following our interpretation). We exclude the formation of a weak C18-H...X hydrogen bond because this atom is not bonded to an oxygen or nitrogen atom. Therefore, alkyl or alkyl-π interactions are suggested. Atom 2 is an atom in ring B that can be C or N (Fig. 5). A high activity at the 5-HT$_{2A}$ receptor is associated with small numerical values for S_{2}^{N}(LUMO+1)*. Table 8 shows that $(LUMO)_{2}^{*}$ has a π character in all cases and that $(LUMO+1)_{2}^{*}$ has π or σ character. Also, $(LUMO)_{2}^{*}$ coincides with molecular MOs close to LUMO. $(HOMO)_{2}^{*}$ has a π nature and it coincides with LUMO or close molecular empty MOs. Within the standard interpretation we need to increase the $(LUMO)_{2}^{*}$ and $(LUMO+1)_{2}^{*}$ energies. For these reasons, we suggest that atom 2 is interacting with an electron-deficient center through its occupied local MOs. The most probable interaction is a π-π one. Atom 11 is a sp^3 carbon in ring C (Fig. 5). Table 8 shows that $(HOMO)_{11}^{*}$ coincides with the molecular HOMO and that $(LUMO)_{11}^{*}$ coincides with empty MOs close to the LUMO. A high activity is associated with large numerical values for S_{11}^{N}(LUMO+2)*. To obtain the values we need to lower $(LUMO+2)_{11}^{*}$ energy, lowering also $(LUMO+1)_{11}^{*}$ and $(LUMO)_{11}^{*}$ energies. Considering that C11 is bonded to N10, our first suggestion is that C11 participates in a non-classical carbon hydrogen bond C11-H…X (X=O or N). In addition, alkyl or alkyl-π interactions are conceivable. Atom 20 is nitrogen in ring D (Fig. 5). A high activity at the 5-HT$_{2A}$ receptor is associated with large (negative) numerical values for S_{20}^{E}(HOMO-2)*. To obtain this large number we must shift $(HOMO-1)_{20}^{*}$ energy toward zero. Table 9 shows that $(HOMO)_{20}^{*}$ coincides with the molecular HOMO or (HOMO-1). This data suggest that atom N20 seems to be involved in a hydrogen bond of the N20…H-O kind. An additional possibility is a π-π interaction. Atom 30 is the atom of the substituent attached to C26 (Fig. 5).

Substituents are H, F, Cl or CN (Table 1). A high activity is associated with large numerical values for S_{30}^{N}(LUMO)*. The nature of the local MOs of the H substituent is σ (Tables 1 and 10). For this case we suggest a C26-H30….X (with X= N, O, S) weak hydrogen bond. Fluorine frontier local MOs have a π character (Table 10) and coincide with molecular MOs close to the molecular HOMO and LUMO. Chlorine and CN frontier MOs also have a π character and coincide with molecular MOs close to the molecular HOMO and LUMO or with the HOMO and LUMO themselves. We suggest that F and Cl engage in a C26-Cl30…X and C26-F30…X halogen interactions. For CN we suggest a π-π interaction. All the suggestions are displayed in the partial 2D pharmacophore of Fig. 19.

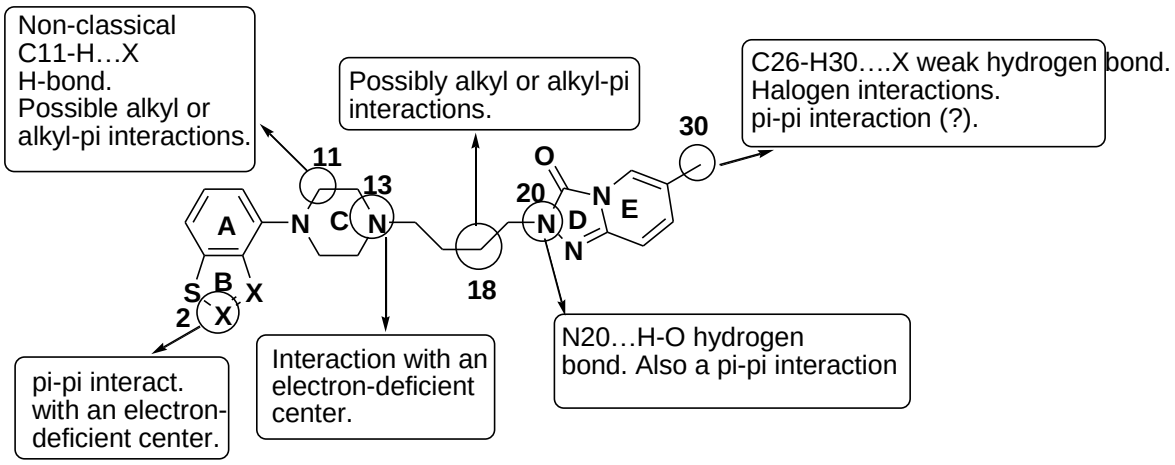

Figure 19: Partial 2D pharmacophore for activity at the 5-HT_{2A} receptor

Discussion of the activity at the D_2 receptor

Table 6 shows that the importance of variables in Eq. 4 is ω_{31}>> S_{30}^{E}(HOMO)*> S_{8}^{N}(LUMO+2)*> F_{31}(LUMO)*> S_{18}^{N}> Q_{26}. A high activity at the D_2 receptor is associated with small numerical values for ω_{31}, large (negative) numerical values for S_{30}^{E}(HOMO)*, large numerical values for S_{8}^{N}(LUMO+2)*, small numerical values for F_{31}(LUMO)*, large numerical values for S_{18}^{N} and a positive net charge on atom 26.

Atom 31 is the atom of the substituent attached to C27 (Fig. 5). Substituents are H or CN (Table 1). A high activity at the D_2 receptor is associated with small numerical values for ω_{31} and F_{31}(LUMO)*. To obtain these small values we must reduce the localization of this MO on atom 31. In other words, the local $(LUMO)_{31}^{*}$ should coincide with molecular empty MOs with high energy. On the other hand, the local atomic electrophilicity is defined as:

$$\omega_{31} = \frac{\mu_{31}^2}{2\eta_{31}} \qquad (6)$$

where μ_{31} is the local atomic electronic potential of atom 31 and η_{31} is the local atomic hardness of atom 31. Remembering that η_{31} is the $HOMO_{31}^{*}$-$LUMO_{31}^{*}$ energy gap, shifting upwards the F_{31}(LUMO)* energy will increase the value of η_{31}, giving a smaller value for ω_{31}. Therefore, both conditions are equivalent. For H atoms it is proposed a weak C27-H31…X (X= N, O, S) hydrogen bond. Perhaps a methyl or ethyl groups should be tested.

Atom 30 is the atom of the substituent attached to C26 (Fig. 5, see also the discussion of this atom presented above). Substituents are H, F, Cl or CN (Table 1). A high activity is associated with large (negative) numerical values for S_{30}^{E}(HOMO)*. This number is obtained by shifting the $(HOMO)_{30}^{*}$ energy toward zero, making this MO more reactive. The local MOs of the H substituent have a σ nature (Table 10). For this case we suggest, as above, a weak C26-H30….X (X= N, O, S) hydrogen bond. Fluorine frontier local MOs have a π character (Table 10) and they coincide with molecular MOs close to the molecular HOMO and LUMO. Chlorine and CN frontier MOs also have a π character and coincide with molecular MOs close to the molecular HOMO and LUMO or with the HOMO and LUMO themselves. We suggest that F and Cl engage in a C26-Cl30…X and C26-F30…X halogen interactions. For CN we suggest a π-π interaction (also, a π-alkyl interaction is possible). Atom 8 is an aromatic carbon in ring A (Fig.

5). A high activity at the D_2 receptor is associated with large numerical values for S_8^N(LUMO+2)*. Large numbers are obtained by shifting the $(LUMO+2)_8^*$ energy towards zero. Table 8 shows that $(HOMO)_8^*$ has a π character and coincides with the molecular HOMO. Also, $(LUMO)_8^*$ has a π character but it coincides with the molecule's (LUMO+1) or (LUMO+2). A high activity at the D_2 receptor is associated with large numerical values for S_{18}^N. From Eq. 5 we know that large numbers are obtained by shifting toward zero the energies of the two or three lowest empty local MOs. Therefore, atom 8 is prone to interact with electron-rich sites such as π regions and/or with anions having π MOs. Atom 18 is a sp^3 carbon in the chain linking rings C and D (Fig. 5). A high activity is associated with large numerical values for S_{18}^N. Table 9 shows that all local MOs have a σ nature, that the local $(HOMO)_{18}$* coincides with the molecular HOMO or (HOMO-1) and that the local $(LUMO)_{18}$* coincides with molecular empty MOs having a higher energy that the LUMO. Given that C18 is not bonded to a nitrogen or oxygen atoms we shall rule out the formation of a weak C18-H...X hydrogen bond. Therefore, we suggest that C18 is participating in alkyl or alkyl-π interactions. Atom 26 is an aromatic carbon in ring D (Fig. 5). A high activity is associated with a positive net charge on atom 26. It is possible that C26 be participating in an electrostatic interaction with a negatively charged center (an anion for example). All the suggestions are displayed in the partial 2D pharmacophore of Fig. 20.

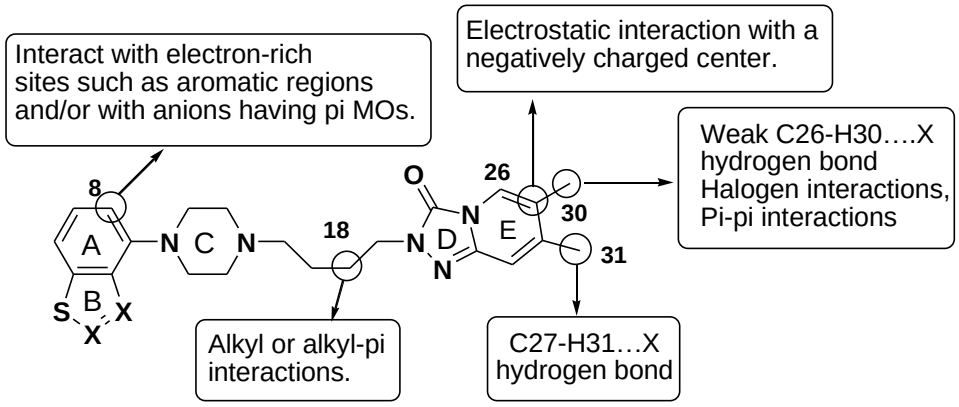

Figure 20: Partial 2D pharmacophore for activity at the D_2 receptor

References

[1]. Wikipedia. Atypical antipsychotic. https://en.wikipedia.org/wiki/Atypical_antipsychotic#Binding_profile (February 1, 2022).

[2]. Singh, S.; Bali, A.; Peshin, T. Synthesis and evaluation of aryl substituted propyl piperazines for potential atypical antipsychotic activity. *Medicinal Chemistry* 2021, 17, 429-441.

[3]. Singh, A.; Bali, A.; Kumari, P. One Pot Synthesis and Pharmacological Evaluation of Aryl Substituted Imidazoles as Potential Atypical Antipsychotics. *Letters in Drug Design & Discovery* 2021, 18, 338-354.

[4]. Gao, L.; Hao, C.; Ma, R.; Chen, J.; Zhang, G.; Chen, Y. Synthesis and biological evaluation of a new class of multi-target heterocycle piperazine derivatives as potential antipsychotics. *RSC Advances* 2021, 11, 16931-16941.

[5]. Watanabe, H.; Ishida, K.; Yamamoto, M.; Horiguchi, M.; Isobe, Y. Synthesis and pharmacological evaluation of 11-(1, 6-dimethyl-1, 2, 3, 6-tetrahydropyridin-4-yl)-5H-dibenzo [b, e][1, 4] diazepines with clozapine-like receptor occupancy at dopamine D1/D2 receptor. *Bioorganic & Medicinal Chemistry Letters* 2020, 30, 127563.

[6]. Shi, W.; Wang, Y.; Wu, C.; Yang, F.; Zheng, W.; Wu, S.; Liu, Y.; Wang, Z.; He, Y.; Shen, J. Synthesis and biological investigation of triazolopyridinone derivatives as potential multireceptor atypical antipsychotics. *Bioorganic & Medicinal Chemistry Letters* 2020, 30, 127027.

[7]. Gao, L.; Yang, Z.; Xiong, J.; Hao, C.; Ma, R.; Liu, X.; Liu, B.-F.; Jin, J.; Zhang, G.; Chen, Y. Design, synthesis and biological investigation of flavone derivatives as potential multi-receptor atypical antipsychotics. *Molecules* 2020, 25, 4107.

[8]. Wu, C.; Wang, Y.; Yang, F.; Shi, W.; Wang, Z.; He, L.; He, Y.; Shen, J. Synthesis and Biological Evaluation of Five-Atom-Linker-Based Arylpiperazine Derivatives with an Atypical Antipsychotic Profile. *ChemMedChem* 2019, 14, 2042-2051.

[9]. Xu, M.; Wang, Y.; Yang, F.; Wu, C.; Wang, Z.; Ye, B.; Jiang, X.; Zhao, Q.; Li, J.; Liu, Y. Synthesis and biological evaluation of a series of multi-target N-substituted cyclic imide derivatives with potential antipsychotic effect. *European journal of medicinal chemistry* 2018, 145, 74-85.

[10]. Xu, M.; Wang, Y.; Yang, F.; Wu, C.; Wang, Z.; Ye, B.; Jiang, X.; Zhao, Q.; Li, J.; Liu, Y. Synthesis and biological evaluation of a series of novel pyridinecarboxamides as potential multi-receptor antipsychotic drugs. *Bioorganic & Medicinal Chemistry Letters* 2018, 28, 606-611.

[11]. Cao, X.; Zhang, Y.; Chen, Y.; Qiu, Y.; Yu, M.; Xu, X.; Liu, X.; Liu, B.-F.; Zhang, L.; Zhang, G. Synthesis and biological evaluation of fused tricyclic heterocycle piperazine (piperidine) derivatives as potential multireceptor atypical antipsychotics. *Journal of medicinal chemistry* 2018, 61, 10017-10039.

[12]. Chen, Y.; Lan, Y.; Wang, S.; Zhang, H.; Xu, X.; Liu, X.; Yu, M.; Liu, B.-F.; Zhang, G. Synthesis and evaluation of new coumarin derivatives as potential atypical antipsychotics. *European journal of medicinal chemistry* 2014, 74, 427-439.

[13]. Gómez-Jeria, J. S.; Ibertti-Arancibia, A. A DFT study of the relationships between electronic structure and dopamine D_1 and D_2 receptor affinity of a group of (S)-enantiomers of 11-(1,6-dimethyl-1,2,3,6-tetrahydropyridin-4-yl)-5*H*-dibenzo[b,e][1,4]diazepines. *Chemistry Research Journal* 2021, 6, 116-131.

[14]. Gómez-Jeria, J. S.; Rojas-Candia, V. A DFT Investigation of the Relationships between Electronic Structure and D_2, 5-HT_{1A}, 5-HT_{2A}, 5-HT_6 and 5-HT_7 Receptor Affinities in a group of Fananserin derivatives. *Chemistry Research Journal* 2020, 5, 37-58.

[15]. Gómez-Jeria, J. S.; Garrido-Sáez, N. A DFT analysis of the relationships between electronic structure and affinity for dopamine D_2, D_3 and D_4 receptor subtypes in a group of 77-LH-28-1 derivatives. *Chemistry Research Journal* 2019, 4, 30-42.

[16]. Gautier, K. S.; Kpotin, G. A.; Mensah, J.-B.; Gómez-Jeria, J. S. Quantum-Chemical Study of the Relationships between Electronic Structure and the Affinity of Benzisothiazolylpiperazine Derivatives for the Dopamine Hd2l and Hd3 Receptors. *The Pharmaceutical and Chemical Journal* 2019, 6, 73-90.

[17]. Gómez-Jeria, J. S.; Valdebenito-Gamboa, J. A Density Functional Study of the Relationships between Electronic Structure and Dopamine D_2 receptor binding affinity of a series of [4-(4-Carboxamidobutyl)]-1-arylpiperazines. *Research Journal of Pharmaceutical, Biological and Chemical Sciences* 2015, 6, 203-218.

[18]. Gómez-Jeria, J. S.; Ojeda-Vergara, M. Electrostatic medium effects and formal quantum structure-activity relationships in apomorphines interacting with D_1 and D_2 dopamine receptors. *International Journal of Quantum Chemistry* 1997, 61, 997-1002.

[19]. Gómez-Jeria, J. S.; Robles-Navarro, A.; Soza-Cornejo, C. A note on the relationships between electronic structure and serotonin 5-HT_{1A} receptor binding affinity in a series of 4-butyl-arylpiperazine-3-(1*H*-indol-3-yl)pyrrolidine-2,5-dione derivatives. *Chemistry Research Journal* 2021, 6, 76-88.

[20]. Gómez-Jeria, J. S.; Gatica-Díaz, N. A preliminary quantum chemical analysis of the relationships between electronic structure and 5-HT_{1A} and 5-HT_{2A} receptor affinity in a series of 8-acetyl-7-hydroxy-4-methylcoumarin derivatives. *Chemistry Research Journal* 2019, 4, 85-100.

[21]. Gómez-Jeria, J. S.; Moreno-Rojas, C. Dissecting the drug-receptor interaction with the Klopman-Peradejordi-Gómez (KPG) method. I. The interaction of 2,5-dimethoxyphenethylamines and their N-2-methoxybenzyl-substituted analogs with 5-HT_{1A} serotonine receptors. *Chemistry Research Journal* 2017, 2, 27-41.

[22]. Gómez-Jeria, J. S.; Abuter-Márquez, J. A Theoretical Study of the Relationships between Electronic Structure and 5-HT_{1A} and 5- HT_{2A} Receptor Binding Affinity of a group of ligands containing an isonicotinic nucleus. *Chemistry Research Journal* 2017, 2, 198-213.

[23]. Gómez-Jeria, J. S.; Castro-Latorre, P.; Moreno-Rojas, C. Dissecting the drug-receptor interaction with the Klopman-Peradejordi-Gómez (KPG) method. II. The interaction of 2,5-dimethoxyphenethylamines and

their N-2-methoxybenzyl-substituted analogs with 5-HT_{2A} serotonine receptors. *Chemistry Research Journal* 2018, 4, 45-62.

[24]. Gómez-Jeria, J. S.; Robles-Navarro, A. DFT and Docking Studies of the Relationships between Electronic Structure and 5-HT_{2A} Receptor Binding Affinity in N-Benzylphenethylamines. *Research Journal of Pharmaceutical, Biological and Chemical Sciences* 2015, 6, 1811-1841.

[25]. Gómez-Jeria, J. S.; Robles-Navarro, A. A Note on the Docking of some Hallucinogens to the 5-HT_{2A} Receptor. *Journal of Computational Methods in Molecular Design* 2015, 5, 45-57.

[26]. Klopman, G. Chemical reactivity and the concept of charge- and frontier-controlled reactions. *Journal of the American Chemical Society* 1968, 90, 223-234.

[27]. Peradejordi, F.; Martin, A. N.; Cammarata, A. Quantum chemical approach to structure-activity relationships of tetracycline antibiotics. *Journal of Pharmaceutical Sciences* 1971, 60, 576-582.

[28]. Gómez Jeria, J. S. La Pharmacologie Quantique. *Bollettino Chimico Farmaceutico* 1982, 121, 619-625.

[29]. Gómez-Jeria, J. S. On some problems in quantum pharmacology I. The partition functions. *International Journal of Quantum Chemistry* 1983, 23, 1969-1972.

[30]. Gómez-Jeria, J. S. Modeling the Drug-Receptor Interaction in Quantum Pharmacology. In *Molecules in Physics, Chemistry, and Biology*, Maruani, J., Ed. Springer Netherlands: 1989; Vol. 4, pp 215-231.

[31]. Gómez-Jeria, J. S.; Ojeda-Vergara, M. Parametrization of the orientational effects in the drug-receptor interaction. *Journal of the Chilean Chemical Society* 2003, 48, 119-124.

[32]. Gómez-Jeria, J. S. *Elements of Molecular Electronic Pharmacology (in Spanish)*. 1st ed.; Ediciones Sokar: Santiago de Chile, 2013; p 104.

[33]. Gómez-Jeria, J. S. A New Set of Local Reactivity Indices within the Hartree-Fock-Roothaan and Density Functional Theory Frameworks. *Canadian Chemical Transactions* 2013, 1, 25-55.

[34]. Gómez-Jeria, J. S.; Flores-Catalán, M. Quantum-chemical modeling of the relationships between molecular structure and in vitro multi-step, multimechanistic drug effects. HIV-1 replication inhibition and inhibition of cell proliferation as examples. *Canadian Chemical Transactions* 2013, 1, 215-237.

[35]. Paz de la Vega, A.; Alarcón, D. A.; Gómez-Jeria, J. S. Quantum Chemical Study of the Relationships between Electronic Structure and Pharmacokinetic Profile, Inhibitory Strength toward Hepatitis C virus NS5B Polymerase and HCV replicons of indole-based compounds. *Journal of the Chilean Chemical Society* 2013, 58, 1842-1851.

[36]. Gómez-Jeria, J. S. Tables of proposed values for the Orientational Parameter of the Substituent. I. Monoatomic, Diatomic, Triatomic, n-CnH2n+1, O-n-CnH2n+1, NRR', and Cycloalkanes (with a single ring) substituents. *Research Journal of Pharmaceutical, Biological and Chemical Sciences* 2016, 7, 288-294.

[37]. Gómez-Jeria, J. S. Tables of proposed values for the Orientational Parameter of the Substituent. II. *Research Journal of Pharmaceutical, Biological and Chemical Sciences* 2016, 7, 2258-2260.

[38]. Gómez-Jeria, J. S. 45 Years of the KPG Method: A Tribute to Federico Peradejordi. *Journal of Computational Methods in Molecular Design* 2017, 7, 17-37.

[39]. Gómez-Jeria, J. S.; Robles-Navarro, A.; Kpotin, G.; Garrido-Sáez, N.; Gatica-Díaz, N. Some remarks about the relationships between the common skeleton concept within the Klopman-Peradejordi-Gómez QSAR method and the weak molecule-site interactions. *Chemistry Research Journal* 2020, 5, 32-52.

[40]. Gómez-Jeria, J. S.; Espinoza, L. Quantum-chemical studies on acetylcholinesterasa inhibition. I. Carbamates. *Journal of the Chilean Chemical Society* 1982, 27, 142-144.

[41]. Gómez-Jeria, J. S.; Morales-Lagos, D. The mode of binding of phenylalkylamines to the Serotonergic Receptor. In *QSAR in design of Bioactive Drugs*, Kuchar, M., Ed. Prous, J.R.: Barcelona, Spain, 1984; pp 145-173.

[42]. Gómez-Jeria, J. S.; Morales-Lagos, D. R. Quantum chemical approach to the relationship between molecular structure and serotonin receptor binding affinity. *Journal of Pharmaceutical Sciences* 1984, 73, 1725-1728.

[43]. Gómez-Jeria, J. S.; Morales-Lagos, D.; Rodriguez-Gatica, J. I.; Saavedra-Aguilar, J. C. Quantum-chemical study of the relation between electronic structure and pA2 in a series of 5-substituted tryptamines. *International Journal of Quantum Chemistry* 1985, 28, 421-428.

[44]. Gómez-Jeria, J. S.; Morales-Lagos, D.; Cassels, B. K.; Saavedra-Aguilar, J. C. Electronic structure and serotonin receptor binding affinity of 7-substituted tryptamines. *Quantitative Structure-Activity Relationships* 1986, 5, 153-157.

[45]. Gómez-Jeria, J. S.; Cassels, B. K.; Saavedra-Aguilar, J. C. A quantum-chemical and experimental study of the hallucinogen (±)-1-(2,5-dimethoxy-4-nitrophenyl)-2-aminopropane (DON). *European Journal of Medicinal Chemistry* 1987, 22, 433-437.

[46]. Gómez-Jeria, J. S.; Sotomayor, P. Quantum chemical study of electronic structure and receptor binding in opiates. *Journal of Molecular Structure: THEOCHEM* 1988, 166, 493-498.

[47]. Gómez-Jeria, J. S.; Ojeda-Vergara, M.; Donoso-Espinoza, C. Quantum-chemical Structure-Activity Relationships in carbamate insecticides. *Molecular Engineering* 1995, 5, 391-401.

[48]. Gómez-Jeria, J. S.; Lagos-Arancibia, L. Quantum-chemical structure-affinity studies on kynurenic acid derivatives as Gly/NMDA receptor ligands. *International Journal of Quantum Chemistry* 1999, 71, 505-511.

[49]. Gómez-Jeria, J. S.; Soto-Morales, F.; Larenas-Gutierrez, G. A Zindo/1 Study of the Cannabinoid-Mediated Inhibition of Adenylyl Cyclase. *Iranian International Journal of Science* 2003, 4, 151-164.

[50]. Soto-Morales, F.; Gómez-Jeria, J. S. A theoretical study of the inhibition of wild-type and drug-resistant HTV-1 reverse transcriptase by some thiazolidenebenzenesulfonamide derivatives. *Journal of the Chilean Chemical Society* 2007, 52, 1214-1219.

[51]. Bruna-Larenas, T.; Gómez-Jeria, J. S. A DFT and Semiempirical Model-Based Study of Opioid Receptor Affinity and Selectivity in a Group of Molecules with a Morphine Structural Core. *International Journal of Medicinal Chemistry* 2012, 2012 Article ID 682495, 1-16.

[52]. Gómez-Jeria, J. S. A quantum chemical analysis of the relationships between electronic structure, PAK1 inhibition and MEK phosphorylation in a series of 2-arylamino-4-aryl-pyrimidines. *SOP Transactions on Physical Chemistry* 2014, 1, 10-28.

[53]. Gómez-Jeria, J. S. A DFT Study of the Inhibition of the Papain-like Protease (PLpro) from the SARS Coronavirus by a Group of 4-Piperidinecarboxamide Derivatives. *Research Journal of Pharmaceutical, Biological and Chemical Sciences* 2014, 5, 424-436.

[54]. Gómez-Jeria, J. S. A Theoretical Study of the Relationships between Electronic Structure and Antifungal Activity against *Botrytis cinerea* and *Colletotrichum lagenarium* of a Group of Carabrone Hydrazone Derivatives. *Research Journal of Pharmaceutical, Biological and Chemical Sciences* 2015, 6, 688-697.

[55]. Gómez-Jeria, J. S.; Gazzano, V. A quantum chemical study of the inhibition of α-glucosidase by a group of oxadiazole benzohydrazone derivatives. *Der Pharma Chemica* 2016, 8, 21-27.

[56]. Gómez-Jeria, J. S.; Latorre-Castro, P. On the relationship between electronic structure and carcinogenic activity in substituted Benz[a]anthracene derivatives. *Der Pharma Chemica* 2016, 8, 84-92.

[57]. Gómez-Jeria, J. S.; Castro-Latorre, P. A Density Functional Theory analysis of the relationships between the Badger index measuring carcinogenicity and the electronic structure of a series of substituted Benz[a]anthracene derivatives. *Chemistry Research Journal* 2017, 2, 112-126.

[58]. Gómez-Jeria, J. S.; Castro-Latorre, P.; Kpotin, G. Quantum Chemical Study of the Relationships between Electronic Structure and Antiviral Activities against Influenza A H1N1, Enterovirus 71 and Coxsackie B3 viruses of some Pyrazine-1,3-thiazine Hybrid Analogues. *International Journal of Research in Applied, Natural and Social Sciences* 2017, 5, 49-64.

[59]. Gómez-Jeria, J. S.; Moreno-Rojas, C.; Castro-Latorre, P. A note on the binding of N-2-methoxybenzyl-phenethylamines (NBOMe drugs) to the 5-HT_{2C} receptors. *Chemistry Research Journal* 2018, 3, 169-175.

[60]. Abdussalam, A.; Gómez-Jeria, J. S. Quantum Chemical Study of the Relationships between Electronic Structure and Corticotropin-Releasing Factor 1 Receptor Binding Inhibition by a Group of Benzazole Derivatives. *Journal of Pharmaceutical and Applied Chemistry* 2019, 5, 1-9.

[61]. Gómez-Jeria, J. S.; González-Ponce, N. A Quantum-chemical study of the relationships between electronic structure and affinities for the serotonin transporter protein and the 5-HT_{1A} receptor in a series of 2H-pyrido[1,2-c]pyrimidine derivatives. *Chemistry Research Journal* 2020, 5, 16-31.

[62]. Gómez-Jeria, J. S.; Robles-Navarro, A.; Soto-Martínez, V. Quantum Chemical Analysis of the relationships between electronic structure and dopamine D_1 and D_5 receptor binding affinities in a series of 1-phenylbenzazepines. *Chemistry Research Journal* 2021, 6, 128-144.

[63]. Gómez-Jeria, J. S.; Soloaga Ardiles, C. E. A Density Functional Theory inquiry of the relationships between electronic structure and anticonvulsant activity in a series of 2,5-disubstituted thiadiazoles. *Chemistry Research Journal* 2022, 7, 55-68.

[64]. Frisch, M. J.; Trucks, G. W.; Schlegel, H. B.; Scuseria, G. E.; Robb, M. A.; Cheeseman, J. R.; Scalmani, G.; Barone, V.; Petersson, G. A.; Nakatsuji, H.; Li, X.; Caricato, M.; Marenich, A. V.; Bloino, J.; Janesko, B. G.; Gomperts, R.; Mennucci, B.; Hratchian, H. P. *Gaussian 16 16Rev. A.03*, Gaussian: Pittsburgh, PA, USA, 2016.

[65]. Gómez-Jeria, J. S. *D-Cent-QSAR: A program to generate Local Atomic Reactivity Indices from Gaussian16 log files*, v. 1.0; Santiago, Chile, 2020.

[66]. Gómez-Jeria, J. S. An empirical way to correct some drawbacks of Mulliken Population Analysis (Erratum in: J. Chil. Chem. Soc., 55, 4, IX, 2010). *Journal of the Chilean Chemical Society* 2009, 54, 482-485.

[67]. Statsoft. *Statistica v. 8.0*, 2300 East 14 th St. Tulsa, OK 74104, USA, 1984-2007.